Figure e-1

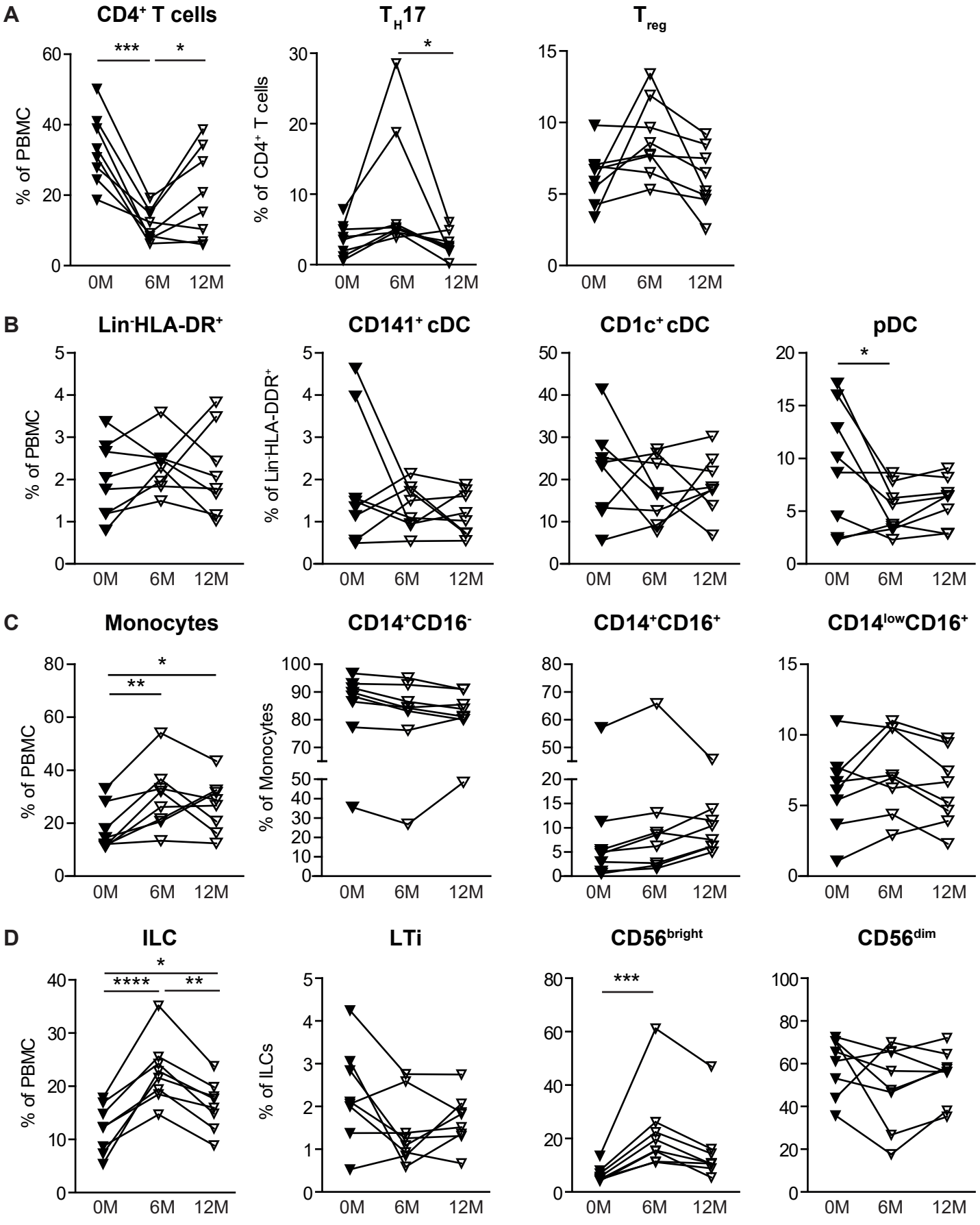

Figure e-1: Alemtuzumab-induced changes in the CD4+ T cell and innate immune cell compartment after 6 and 12 months. (A) Graphs displaying proportions of CD4+ T cell subsets derived from alemtuzumab treated RRMS patients (n=8) at baseline (filled triangles) and follow-up at 6-months and 12-months (open triangles). (B) Graphs displaying proportions of DC subsets derived from alemtuzumab treated RRMS patients (n=8) at baseline (filled triangles) and follow-up at 6-months and 12-months (open triangles). (C) Graphs displaying proportions of monocyte subsets derived from alemtuzumab treated RRMS patients (n=8) at baseline (filled triangles) and follow-up at 6-months and 12-months (open triangles). (D) Graphs displaying proportions of ILC subsets derived from alemtuzumab treated RRMS patients (n=8) at baseline (filled triangles) and follow-up at 6-months and 12-months (open triangles). P-values were calculated by RM-ANOVA with Bonferroni post-test, *p<0.05, **p<0.01, ***p<0.001, ****p<0.0001.

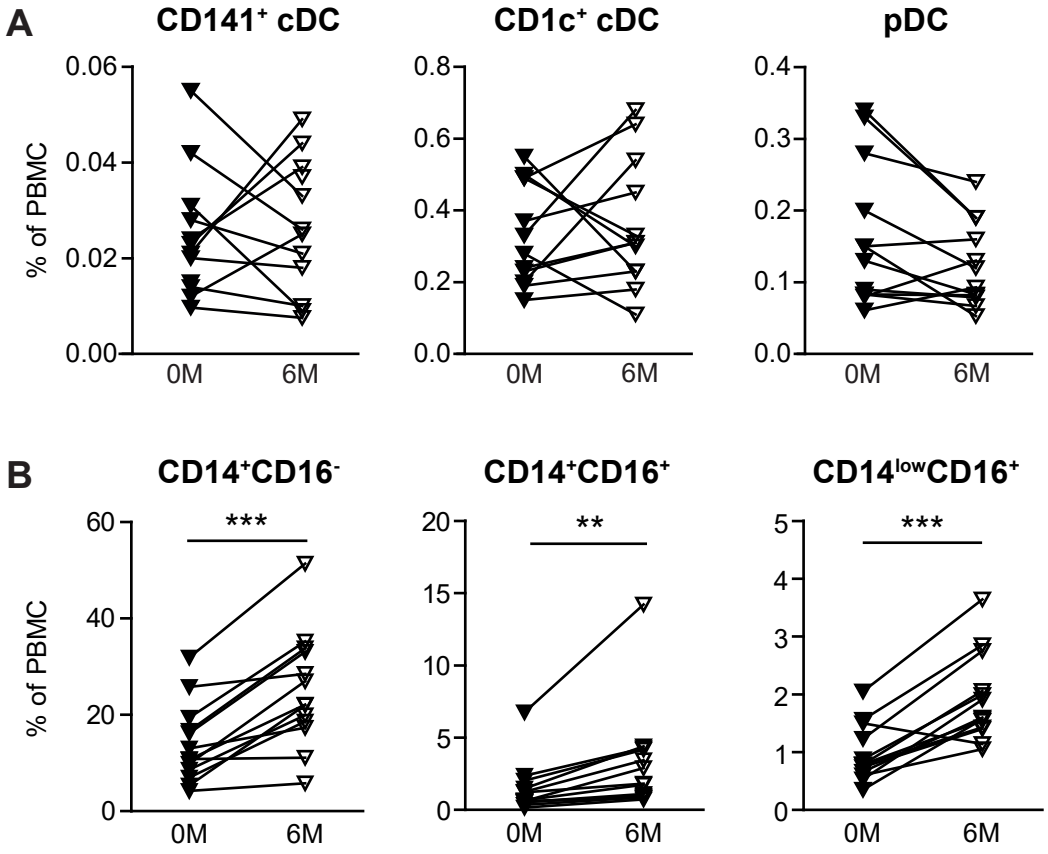

Figure e-2: Alemtuzumab-induced changes in the myeloid cell compartment. Graphs displaying PBMC proportions of (A) DC subsets and (B) monocyte subsets derived from alemtuzumab treated RRMS patients (n=12) at baseline (filled triangles) and follow-up at 6-months (open triangles). P-values were calculated by paired student τ-test or Wilcoxon matched-pairs signed rank test, respectively, *p<0.05, **p<0.01, ***p<0.001.

Figure e-3

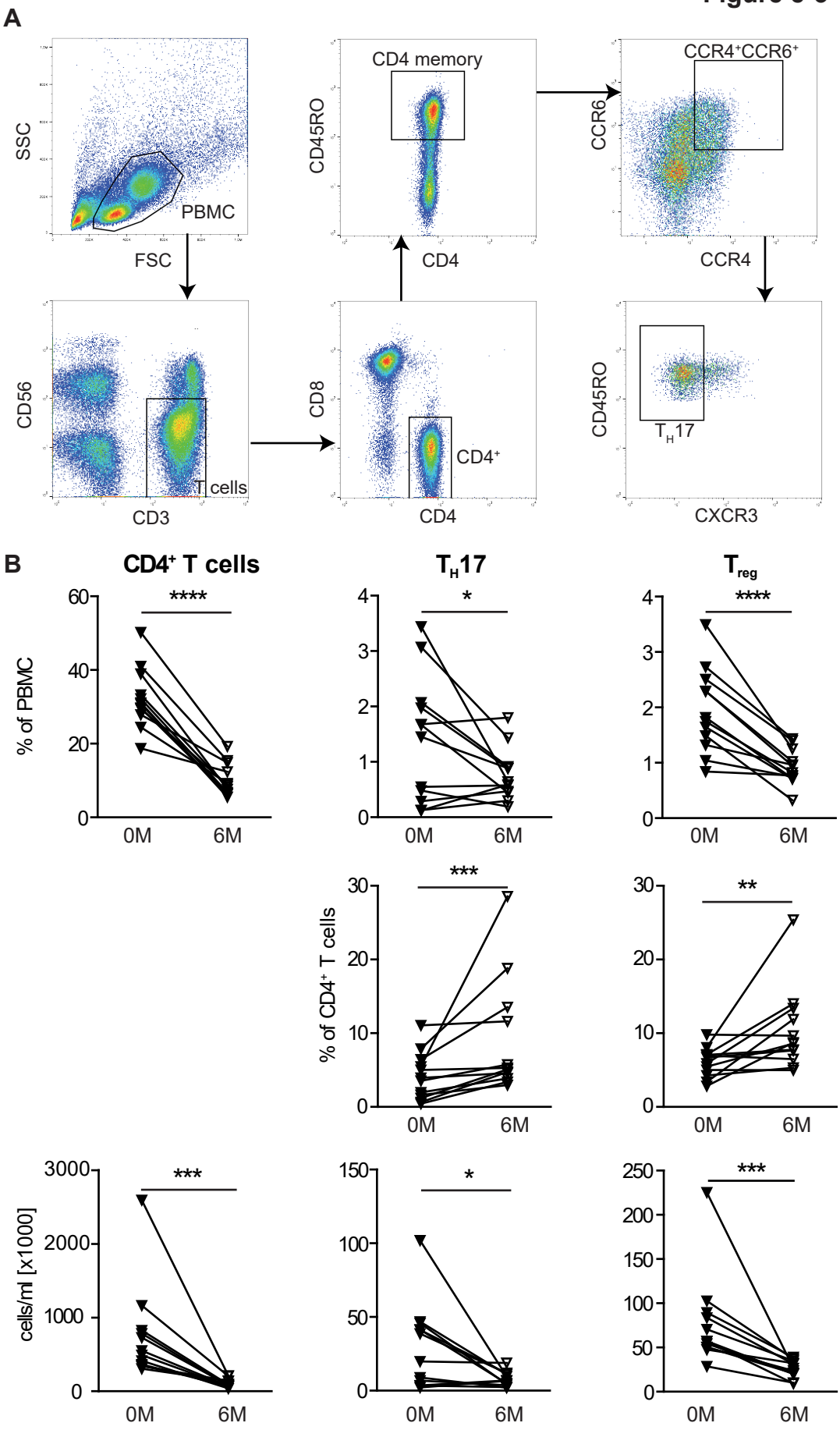

Figure e-3: Alemtuzumab-induced changes in the CD4⁺ T cell compartment. (A) Gating strategy for T cell subsets. PBMCs were gated by FSC vs. SSC characteristics. T cells were selected based on the expression of CD3 and the absence of CD56. $CD4^+CD8^-CD45RO^+$ memory T cells were gated into $CCR4^+CCR6^+CXCR3^-$ TH17 cells, as described in literature.[1] (B) Graphs displaying proportions within PBMCs (upper row), within CD4⁺ T cells (middle row), and total cell numbers (lower row) of CD4⁺ T cell subsets derived from alemtuzumab treated RRMS patients (n=12) at baseline (filled triangles) and 6-month follow-up (open triangles). P-values were calculated by paired student τ-test or Wilcoxon matched-pairs signed rank test, respectively, *p<0.05, **p<0.01, ***p<0.001, ****p<0.0001.

[1] Zielinski CE, Mele F, Aschenbrenner D, et al. Pathogen-induced human TH17 cells produce IFN-gamma or IL-10 and are regulated by IL-1beta. Nature 2012;484:514-518.

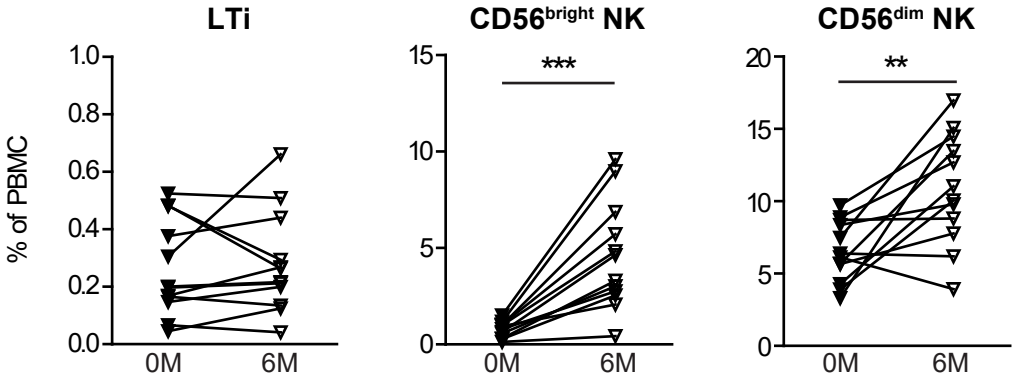

Figure e-4: Alemtuzumab-induced changes in the innate lymphoid cell compartment. Graphs displaying proportions of ILC subsets among PBMCs derived from alemtuzumab treated RRMS patients (n=12) at baseline (filled triangles) and at 6-month follow-up (open triangles). P-values were calculated by paired student τ-test or Wilcoxon matched-pairs signed rank test, respectively, *p<0.05, **p<0.01, ***p<0.001.

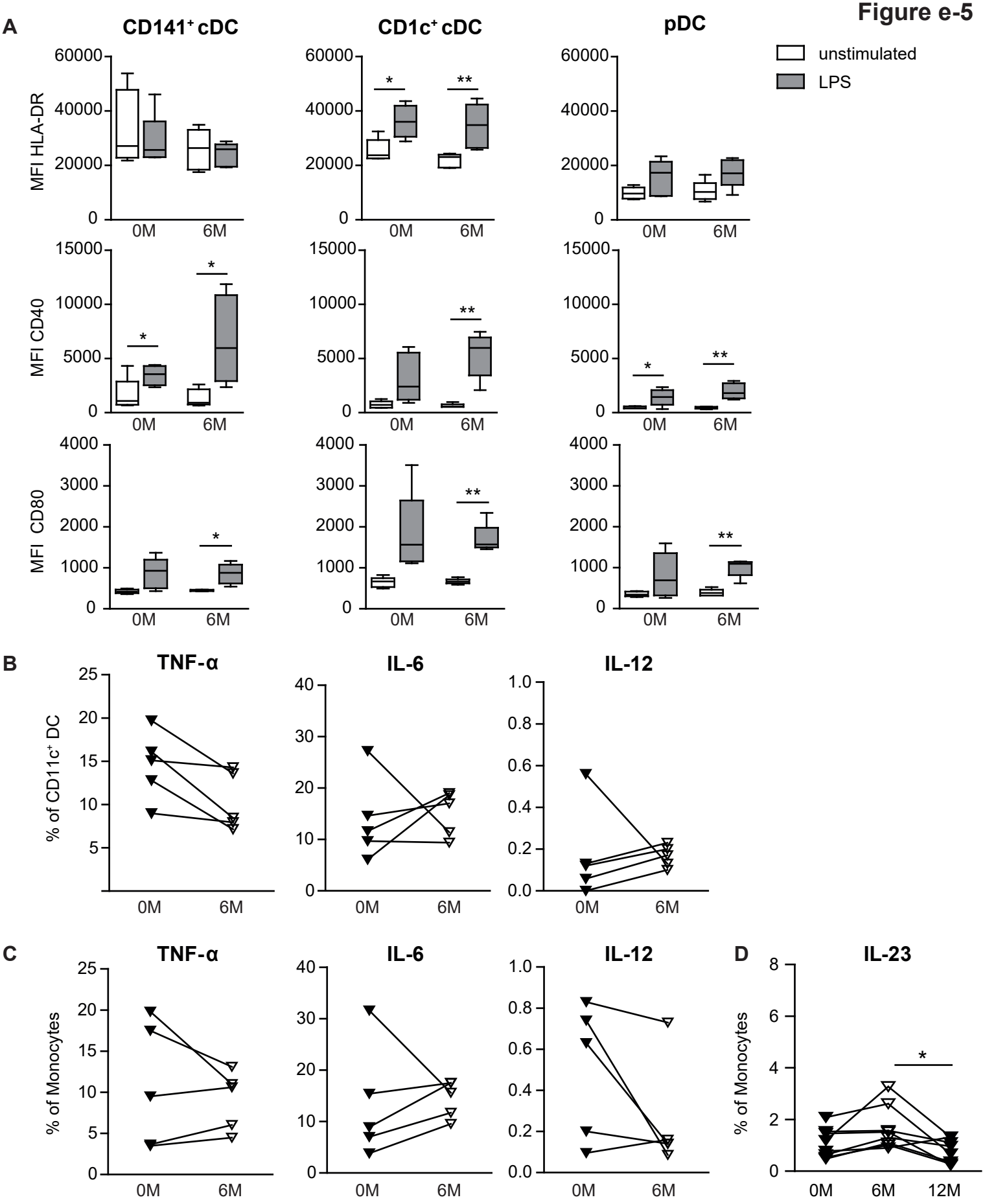

Figure e-5: Expression of maturation markers and cytokine production by myeloid cells after alemtuzumab treatment. (A) Graphs displaying the MFI of HLA-DR (upper row), CD40 (middle row) and CD80 (bottom row) of conventional CD141⁺ and CD1c⁺ DCs and pDCs in unstimulated (open boxes) and LPS-stimulated (closed boxes) condition. (B) Graphs displaying proportions of cytokine producing DCs at baseline (closed triangles) and 6 months (open triangles) after alemtuzumab therapy. (C) Graphs displaying proportions of cytokine producing monocytes at baseline and 6 months after alemtuzumab therapy. PBMCs were derived from alemtuzumab treated RRMS patients (n=5) at baseline (0M) and 6-month follow-up (6M). (D) Graphs displaying proportions of IL-23 producing monocytes (n=8) at baseline and 6 and 12 months after alemtuzumab therapy. P-values were calculated by paired student τ-test (A-C) and with RM-ANOVA with Bonferroni post-test (D), *p<0.05, **p<0.01.